Modeling 2D and 3D of Hybrid Laser Nd:Yag - MIG Welding Processes

E. Le Guen[*,1], R. Fabbro[1], F. Coste[1], M. Carin[2] and P. Le Masson[2]
[1] LALP (CNRS)/GIP GERAILP, 16 bis Av. Prieur de la Côte d'Or 94114 ARCUEIL Cedex France,
[2] LIMATB, Université de Bretagne Sud, Centre de recherche de Saint Maudé, BP 92116, 56321 LORIENT Cedex France
*Corresponding author: LALP (CNRS)/GIP GERAILP, 16 bis Av. Prieur de la Côte d'Or 94114 ARCUEIL Cedex France, eleguen@gerailp.fr

Abstract: Hybrid laser-MIG arc welding has very interesting advantages compared to laser welding or arc welding used separately. It is known that improvement of productivity results in higher welding speeds, thicker welded materials, joint fit-up allowance, better stability of molten pool, and improvement of joint metallurgical quality. In order to use efficiently these techniques in industrial production, it is necessary to precisely understand the complex physical phenomena that govern this welding process. This paper intends to present numerical simulations of thermal phenomena in the molten bath, obtained with a 2D hydrodynamic model and 3D thermal model of Hybrid laser-MIG arc welding process. The 3D model comprises the calculation of the deformed weld pool profile.

Keywords: laser hybrid Nd:Yag, MIG welding, modelling, thermohydraulic flow

1. Introduction

Despite its limitations, gas metal arc (GMA) welding is a very interesting process that is widely used nowadays in industry. However, hybrid welding that combines laser keyhole welding and arc welding with addition of filler wire begins also to be seriously used because its provides essential advantages. Deep penetration allows the welding of rather thick materials even at high welding speeds allowing filling of unavoidable gaps of the joints, with possible improved metallurgical properties and controlled geometry of the weld seam. It is known that the strength of a weld seam is controlled by many parameters. Its geometry is one of these crucial parameters that have to be controlled or even optimised if one wants to minimize the effect of induced stress field generated during loading cycles of these welds. Similarly the metallurgical properties of these welds are also depending of the thermal cycles induced by the involved heat sources, the arc and the laser, which are used during this process. Experimental approaches are presently adapted in order to obtain corresponding data on these resulting characteristics, but of course they are limited to the range of the operating parameters that are used. Moreover, this hybrid process is rather complex and no satisfactory complete understanding is available. We know that each process alone is not already completely mastered or understood, as of course their combination. Therefore, the development of a mathematical modelling of this hybrid process that would take into account the main involved physical processes would be a very useful tool for estimating the final parameters of the weld seam for a given set of operating parameters. Different studies have already approached several aspects of this process [1-2]; they concern the study of some specific physical processes such as for example, dynamic generation and interaction of the droplets with the melt and resulting transport phenomena inside in melt pool. GMA welding process alone has also been studied by using heat and fluid flow inside a 3-D model of melt pool [3].

In this paper we present the first results of a numerical model of hybrid laser-GMA welding. This model is able to predict the 3D geometry of the weld reinforcement observed at the top and root drop-out at the bottom of welded samples. The equation of energy is then solved in this deformed geometry. Our goal here is to define a numerical tool that is rather easy to run and enough precise in order to determine these geometrical considerations.

These simulations are validated with corresponding experimental observations. The numerical approach will be described in three parts with experimental comparison: 3D thermal approach, description of the deformation on free surface and hydrodynamic approach. The influence of various parameters such as energy density, their distribution over the shape of the weld pool as well as the temperature and velocity fields on the weld pool, are shown through several cases of calculations.

2. Experimental setup

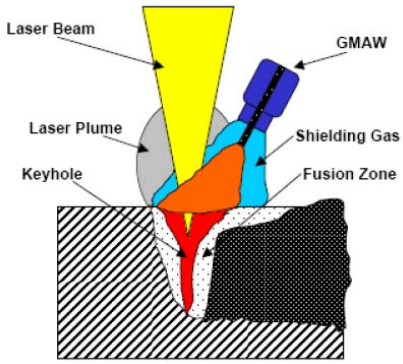

Figure 1 : Schematic of the Hybrid laser-MIG welding process

Figure 1 shows a schematic sketch of the hybrid laser-MIG welding process. Experiments were carried out with a CW Nd:Yag 4006D TRUMPF Laser, with a maximum power of 4 kW. The laser beam was delivered through a 600 µm optical fibre. The welding head images the exit of the optical fibre by using a collimating and focusing lens of 200 mm focal distance. A focal spot of 600 microns is thus generated and the focal spot intensity distribution was analysed by using a PROMETEC beam analyser. It confirmed that the intensity distribution could be considered as "top-hat".
The arc torch is a DIGI WAVE 400 model from SAFT PRO (Air Liquide Welding France). It delivers up to 400 A current for different configurations of control of current and tension of the arc. Several shielding gas were used, they mainly consist of pure Argon or Arcal21 (92% Ar and 8% of CO2). Of course, it is possible to vary all the geometric parameters of the torch (position and wire angle with the vertical laser beam).
The dynamics of the melt pool was analysed with a CMOS fast camera (PHOTRON IMAGER FASTCAM APX RS 3000) with a maximum recording rate of 30 kHz. Lateral observations of the melt pools geometry were realized by placing this camera on the side, perpendicularly to the welding displacement, with the optical axis of the camera making an angle of 40° with the vertical of the incident laser beam.

3. 3D Thermal Approach

In a first step, a 3D heat conduction model was developed to simulate the laser welding process. For the description of the laser keyhole welding we used the previous analysis of Lankalapalli et al. [4]. In this approach, the keyhole is assumed cylindrical with a uniform temperature along its wall. This temperature is set here at a value slightly above the evaporation temperature of the used material. The laser power is supposed to be completely absorbed by the wall of the keyhole. The depth of the keyhole is then determined iteratively such that the integral of the heat flux along the entire surface wall is equal to the total absorbed laser power. An analytical description can also be used for that determination in the case of constant material properties. The diameter of the keyhole is supposed to be equal to the diameter of the laser spot at the focus point, which is in agreement with experiments.
As the system includes a symmetry plane, only a half-piece is considered. The work piece studied here consists in a stainless steel 316L plate of any dimension (variable length, width, thickness as required by the study) with a cylindrical hole representing the keyhole generated by the laser irradiation. The initial temperature T_0 is equal to 300 K. The material properties are temperature-dependant and the latent heat of fusion is taken into account. The work piece is irradiated by the laser perpendicularly to the surface and moving at a velocity of U_0 along x-axis. The welding problem is assumed to be at a quasi-steady state.
In this first model, the hydrodynamics phenomena are not taken into account. The energy equation is solved using a coordinate system moving with the heat source and can be written as:

$$\rho C_p U_0 \frac{\partial T}{\partial x} = \frac{\partial}{\partial x}\left(\lambda \frac{\partial T}{\partial x}\right) + \frac{\partial}{\partial y}\left(\lambda \frac{\partial T}{\partial y}\right) + \frac{\partial}{\partial z}\left(\lambda \frac{\partial T}{\partial z}\right)$$

where ρ represents the density, C_p the effective heat capacity, U_0 the welding velocity, λ the thermal conductivity and T the temperature.
An example of comparison between experiments and corresponding simulations is shown in Figure 2. With the operating parameters used in experiment, the melted section can be correctly reproduced when a total laser power of 2.8 kW is

absorbed at the keyhole wall with a temperature of 4000K. This absorbed power of 2.8 kW has to be compared with the corresponding incident experimental one of 3.8 kW. The discrepancy is interpreted by the unstationary observed behaviour of the keyhole that undergoes strong closing fluctuations probably resulting from Rayleigh-Taylor instability for these low welding speed regimes [5]. At higher welding speeds, this behaviour is strongly reduced, the observed discrepancy is then efficiently reduced.

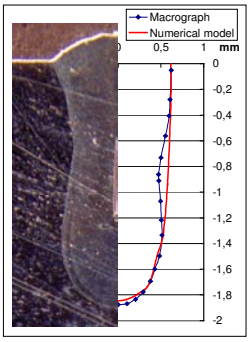

Figure 2 : Comparison between a cross section obtained with keyhole laser welding and corresponding simulations (P_{laser}= 4 kW, U_0 = 6m/min)

This first model was also applied to simulate the hybrid laser-MIG arc welding process. In that case, a Gaussian heat source is added at the top of the work piece to represent the arc energy, which is expressed as follows:

$$\varphi_{MIG} = \frac{\eta U I}{2\pi r_q^2} \exp\left(-\frac{(x+d)^2 + y^2}{2 r_q^2}\right)$$

where η is the arc efficiency, U is the voltage, I is the current, r_q is the heat distribution parameter and d is the distance between the arc center line and the keyhole.

Figure 3 shows a comparison between a cross section obtained with MAG welding and corresponding simulations. It is found that the weld pool shape cannot be predicted with accuracy. Indeed, the energy distribution of the arc is assumed to be deposit on a flat surface, whereas in experiment the top surface of the weld pool is deformed. This justifies our further development concerning the calculation of the deformed surface of the weld pool.

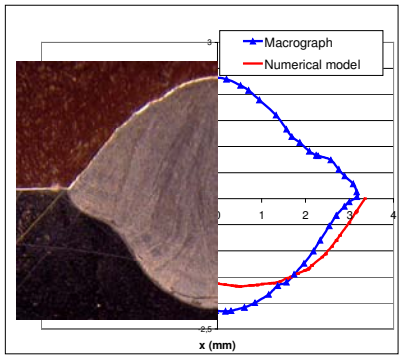

Figure 3 : Comparison between a cross section obtained with MAG and corresponding simulations (U_0=1m/min, ηUI=4.2 kW)

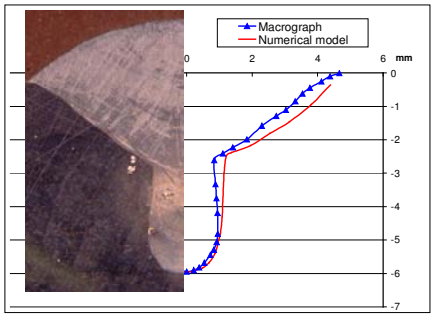

Figure 4 : Comparison between a cross section obtained with Laser-MAG conditions and corresponding simulations Hybrid (P_{laser}: 4 kW, U_0 = 10m/min, arc conditions: see text)

In the case of hybrid conditions (Figure 4), the experimental observations can be satisfactorily reproduced even if the melt reinforcement is not taken into account here. The parameters of the Gaussian distribution of the arc heating used here correspond to an electrical power ηUI=4.2 kW (U = 22V, I = 190 A, η≈ 0.7) with a 1/√e radius r_q=2.5 mm (see Fig. 5). These parameters could also be roughly applied for different welding speeds.

This first model was also used to verify another interesting experimental observation concerning the effect of the distance between the arc center line and the keyhole on the keyhole penetration. In Figures 5 and 6, it can be seen that when the arc is in a leading position the keyhole penetration can be significantly increased by more than 20%: in that case, the preheating effect of the arc heating around the keyhole makes the local heat flux from keyhole

surface smaller, and so more incident laser power is available for a deeper penetration.

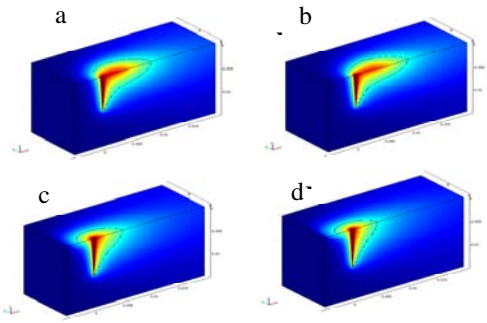

Figure 5 : 3D Simulation of Hybrid Laser-MAG welding (P_{laser}= 4 kW, ηUI = 4kW, U_0 = 1m/min)
a) d = 2 mm (trailing position), b) d = 3 mm (trailing position), c) d = 2 mm (leading position), d) d = 2 mm (leading position)

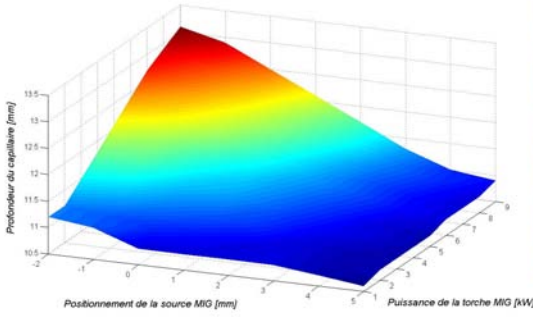

Figure 6 : Keyhole penetration depth (vertical Z axis) as a function of distance d between arc center line and keyhole (horizontal X axis) (negative values: leading arc) and MIG power (horizontal, Y axis)

4. Surface deformation

High speed video movies have shown the depression of the melt pool below the arc followed by weld reinforcement due to the melting of filler wire. In that case the weld pool surface has a shape that must satisfy an equilibrium condition between surface tension, hydrostatic pressure and arc pressure. Ushio and Wu [3] have previously proposed a solution of this problem to predict the weld pool geometry in gas metal arc. This work is based on a variational approach that minimizes the total energy of the melt pool, with the constraints that the melt pool has a constant volume and weld reinforcement geometry is defined by the filler wire mass flow. The energy of the melt pool taken into account concerns the variation of surface energy with a corresponding change of its area, the total potential energy inside the gravitational field, and the work performed during that change of area by the arc pressure and droplets flow momentum. We have adapted this approach to predict the weld pool deformation in hybrid laser-MAG welding [6] by developing an algorithm using the Comsol/Matlab software.

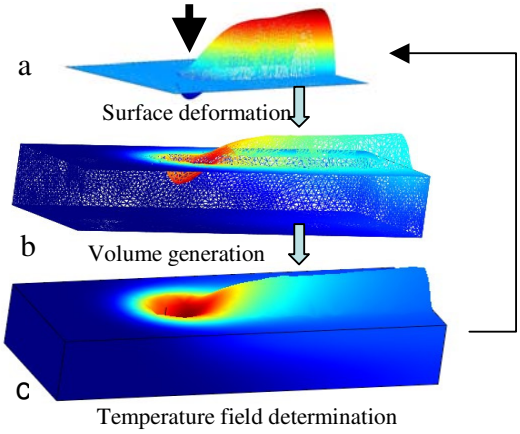

Figure 7 : Principle of algorithm implementation for 3-D description of melt pool.

Figure 7 shows the different steps used in the algorithm:
1) For an initially given isotherm at melting temperature, the deformed profile of the melt pool inside this isotherm is computed using the previous variational method.
2) A 3-D volume is then created in which the top surface coincides with the deformed profile calculated in step 1.
3) The thermal field is computed on this 3D volume.
4) The resulting isotherm at melting temperature is then compared with the one used in step 1, and the entire process is repeated until convergence is obtained.

Figure 8 shows an example of the resulting profiles. The comparison with an experimental result obtained from a steel sample (S355) is rather satisfactory despite our simplifying assumptions.

a)

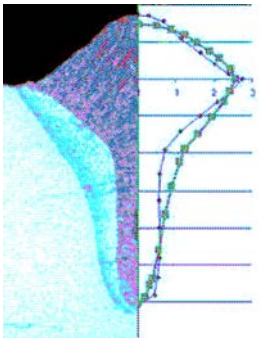

b)

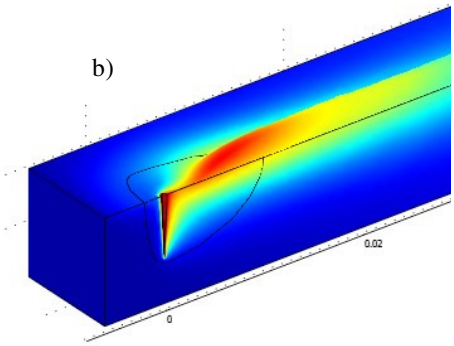

Figure 8 : a) Comparison of cross-section obtained with a hybrid laser-MAG welding and simulation (red square).
b) Temperature field in hybrid laser-MAG process (leading laser).

5. 2D Hydrodynamic Approach

In our previous models, the hydrodynamics phenomena were neglected. However these phenomena can strongly affect the weld pool shape. Because of the complexity of the hybrid welding, we have first developed a 2D hydrodynamic model to simulate the fluid flow around the keyhole. The liquid metal is considered as an incompressible Newtonian fluid.

The equations of mass and momentum conservation are supposed to govern the fluid flow:

$$\frac{\partial u}{\partial x}+\frac{\partial v}{\partial y}=0$$

$$\rho\left((u-U_0)\frac{\partial u}{\partial x}+v\frac{\partial u}{\partial y}\right)=-\frac{\partial p}{\partial x}+\mu\left(\frac{\partial^2 u}{\partial x^2}+\frac{\partial^2 u}{\partial y^2}\right)+S_u$$

$$\rho\left((u-U_0)\frac{\partial v}{\partial x}+v\frac{\partial v}{\partial y}\right)=-\frac{\partial p}{\partial y}+\mu\left(\frac{\partial^2 v}{\partial x^2}+\frac{\partial^2 v}{\partial y^2}\right)+S_v$$

where $S_u = K u$, $S_v = K v$ and $K = -C\frac{(1-f_L)^2}{f_L^3+b}$

The energy equation is given as:

$$\rho C_p\left(u\frac{\partial T}{\partial x}+v\frac{\partial T}{\partial y}\right)=\frac{\partial}{\partial x}\left(\lambda\frac{\partial T}{\partial x}\right)+\frac{\partial}{\partial y}\left(\lambda\frac{\partial T}{\partial y}\right)$$

In figure 9, we compare the weld pool shape calculated by the hydrodynamic model with a purely conductive model. We observe a slight difference in weld pool length which is smaller in the hydrodynamic model. This can be explained by the flow pattern behind the keyhole, as shown in figure.10. Moreover no significant difference has been observed on the weld pool width. In the present study, we refer to a configuration of low speed welding (few m/min). The influence of hydrodynamic is negligible. A 3D hydrodynamic model is being under development to confirm the results obtained in 2D. But it faces problems of computer performance.

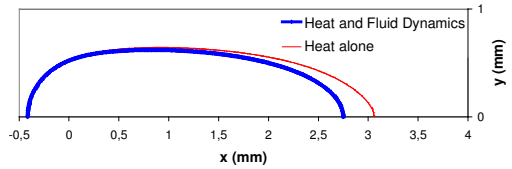

Figure 9 : Weld pool shape comparison

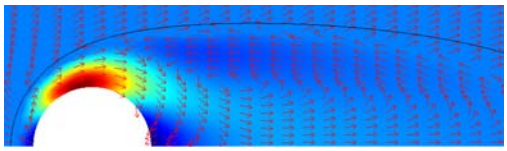

Figure 10 : Velocity field

Conclusion

This paper presents preliminary results concerning the modeling of the hybrid laser-MIG/MAG process. We have obtained encouraging results by using rather simplifying approaches and assumptions. Future developments will consider a better description of physical processes and particularly the weld

seam behavior when gaps of different shapes between the sheets are used. Also, for having direct comparisons with corresponding modeling we have to precisely determine, by using laser profilometry techniques, the exact profile of the weld seam in the depression region and during its transition to the weld reinforcement. These data should be of course obtained on a rather large range of operating parameters. Also the parameters related to the dynamics of the emitted droplets from the filler wire (size, velocity, frequency of detachment) should be clarified for our experimental conditions. Measurement of temperature profiles (by using thermocouples or thermal camera) should be also necessary for having more experimental comparisons. Concerning the evolution of the modeling, next step will consist in describing 3D hydrodynamic flow inside the melt pool and thermocapillary effects, in order to see their consequences on melt pool geometry. It is clear that these developments will make the handling of these modeling less practical and easy compared to what has been presented here.

References

[1] Zhou J., Tsai H.L., (2008) modelling of transport phenomena in hybrid laser-MIG keyhole welding, Heat mass Transfer, doi:10.1016/j.ijheatmasstransfer.2008.02.011

[2] Lin Q., Li X., Simpson S.W., (2001) Metal transfer measurements in gas metal arc welding, J. Phys. D:Appl. Phys. **34**, 347-353

[3] Ushio M., Wu C. S. (1997) Mathematical modelling of three-dimensional heat and fluid flow in a moving gas metal arc weld pool, Metallurgical and materials transactions B, 28B, 509-516.

[4] Lankalapalli K. N., Tu J. F., Gartner G. (1996) A model for estimation penetration depth of laser welding processes, J. Phys. D: Appl. Phys. **29**, 1831-1841

[5] Fabbro, (2002) Basic processes in deep penetration laser welding, Proceedings of the ICALEO'2002 Conference, Scottsdale, USA Oct. 14-17.

[6] Chauvet C., Launay J., Le Masson P., Carin M., Modélisation du soudage hybride, Proceedings of « Club Laser et Procédés » Conference, Rennes (France) June 18-20.